

Polarizations in $B \rightarrow VV$ decays

Hsiang-nan Li^{1*} and Satoshi Mishima^{2†}

¹*Institute of Physics, Academia Sinica, Taipei, Taiwan 115, Republic of China*

¹*Department of Physics, National Cheng-Kung University,
Tainan, Taiwan 701, Republic of China*

²*Department of Physics, Tohoku University, Sendai 980-8578, Japan*

PACS index : 13.25.Hw, 11.10.Hi, 12.38.Bx

Abstract

We demonstrate that the polarization fractions of most tree-dominated $B \rightarrow VV$ decays can be simply understood by means of kinematics in the heavy-quark or large-energy limit. For example, the longitudinal polarization fractions R_L of the $B^0 \rightarrow (D_s^{*+}, D^{*+}, \rho^+) D^{*-}$ and $B^+ \rightarrow (D_s^{*+}, D^{*+}, \rho^+) \rho^0$ modes increase as the masses of the mesons D_s^{*+}, D^{*+}, ρ^+ emitted from the weak vertex decrease. The subleading finite-mass or finite-energy corrections modify these simple estimates only slightly. Our predictions for the $B \rightarrow D_{(s)}^* D^*$ polarization fractions derived in the perturbative QCD framework, especially $R_L \sim 1$ for $B^0 \rightarrow \bar{D}^{*0} D^{*0}$ governed by nonfactorizable W -exchange amplitudes, can be confronted with future data. For penguin-dominated modes, such as $B \rightarrow \rho(\omega) K^*$, the polarization fractions can be understood by the annihilation effect from the $(S-P)(S+P)$ operators, plus the interference with a small tree amplitude. At last, we comment on the various mechanism proposed in the literature to explain the abnormal $B \rightarrow \phi K^*$ polarization data, none of which are satisfactory.

*E-mail: hnli@phys.sinica.edu.tw

†E-mail: mishima@tuhep.phys.tohoku.ac.jp

1 INTRODUCTION

The measured polarization fractions in the $B \rightarrow \phi K^*$ decays have exhibited an anomaly. Let $R_{L,\parallel,\perp}$ denote the longitudinal, parallel, and perpendicular polarization fractions of a $B \rightarrow VV$ mode, respectively. It is well known from a helicity argument that these fractions for light vector mesons V follow the naive counting rules,

$$R_L \sim 1 - O(m_V^2/m_B^2), \quad R_{\parallel} \sim R_{\perp} \sim O(m_V^2/m_B^2), \quad (1)$$

if the emission topology of diagrams dominates, where m_B (m_V) is the B (V) meson mass. That is, Eq. (1) holds for tree-dominated modes, such as $B \rightarrow \rho\rho$, whose longitudinal polarization fraction has been observed to be $R_L \sim 1$ [1, 2]. For penguin-dominated modes, Eq. (1) could be modified by annihilation contributions to some extent [3, 4]. However, the $B \rightarrow \phi K^*$ polarization fractions shown in Table 1 were found to dramatically differ from the naive counting rules, and have been considered as a puzzle.

Mode	Pol. Fraction	Belle	Babar
$B^+ \rightarrow \phi K^{*+}$	R_L	$0.49 \pm 0.13 \pm 0.05$ [5]	$0.46 \pm 0.12 \pm 0.03$ [2]
	R_{\perp}	$0.12^{+0.11}_{-0.08} \pm 0.03$ [5]	
$B^0 \rightarrow \phi K^{*0}$	R_L	$0.52 \pm 0.07 \pm 0.05$ [5]	$0.52 \pm 0.05 \pm 0.02$ [6]
	R_{\perp}	$0.30 \pm 0.07 \pm 0.03$ [5]	$0.22 \pm 0.05 \pm 0.02$ [6]
Mode	Pol. Fraction	Belle	Babar
$B^+ \rightarrow \rho^0 K^{*+}$	R_L		$0.96^{+0.04}_{-0.15} \pm 0.04$ [2]
$B^+ \rightarrow \rho^+ K^{*0}$	R_L	$0.50 \pm 0.19^{+0.05}_{-0.07}$ [7]	$0.79 \pm 0.08 \pm 0.04 \pm 0.02$ [8]

Table 1: Polarization fractions in the penguin-dominated $B \rightarrow VV$ decays.

In this work we shall investigate all the $B \rightarrow VV$ polarization data carefully, and understand more the above puzzle. We show that the $B \rightarrow VV$ modes can be classified into four categories: the first category can be easily understood by means of kinematics in the heavy-quark limit. Take the $B^0 \rightarrow (D_s^{*+}, D^{*+}, \rho^+) D^{*-}$ modes as examples. Under the naive factorization assumption (FA) [9], QCD dynamics in different helicity amplitudes is absorbed into the universal Isgur-Wise (IW) function [10]. The polarization fractions are then completely determined by the kinematic factors, leading to the observation that R_L increases from 0.5 to 0.9, when the vector mesons from the weak vertex change through D_s^* , D^* and ρ . We shall examine sub-leading effects by deriving the perturbative QCD (PQCD) [11, 12] factorization formulas for the $B \rightarrow D_{(s)}^* D^*$ decays up to next-to-leading power in $m_{D_{(s)}^*}/m_B$, m_{D^*} being the $D_{(s)}^*$ meson mass. To this level of accuracy, the various form factors deviate from the IW function, and the nonfactorizable contributions appear. It will be demonstrated that the simple kinematic estimates are robust under these subleading corrections. As a byproduct, we observe that $R_L \sim 1$ for $B^0 \rightarrow \bar{D}^{*0} D^{*0}$, governed by nonfactorizable W -exchange amplitudes, differs from $R_L \sim 0.5$ for other $B \rightarrow D^* D^*$ modes. This PQCD prediction can be confronted with data in the future.

The second category is understandable via kinematics in the large-energy limit, which consists of tree-dominated B meson decays into light vector mesons, such as $B \rightarrow (\rho, \omega)\rho$. Their

helicity amplitudes can be expressed in terms of various heavy-to-light transition form factors under FA, which are related to each other by the large-energy symmetry relations. It turns out that only two universal form factors associated with the longitudinally and transversely polarized final states are relevant. If these two form factors do not differ much, the polarization fractions will be completely determined by the kinematic factors, leading to $R_L \sim 1$ consistent with Eq. (1). The same argument applies to the $B^+ \rightarrow (D_s^{*+}, D^{*+})\rho^0$ decays with the D_s^{*+}, D^{*+} mesons being emitted from the weak vertex, whose $R_L \sim 0.7$ are predicted, and can be compared with the future data. We then examine subleading corrections to the large-energy symmetry relations by including the two-parton twist-4 contribution. Adding this piece to the longitudinal polarization amplitude makes complete the next-to-leading-power analysis at two-parton level, since the transverse polarization amplitudes are of next-to-leading power by themselves. It will be demonstrated that this subleading effect is also negligible.

The third category contains penguin-dominated modes, such as $B \rightarrow \rho(\omega)K^*$, which can exhibit a sizable deviation from the naive counting rules in Eq. (1). As shown in [3], the annihilation amplitudes associated with the $(S-P)(S+P)$ operators follow the counting rules,

$$R_L \sim R_{\parallel} \sim R_{\perp} . \quad (2)$$

The PQCD analysis has indicated that the penguin annihilation contribution, together with nonfactorizable corrections, bring the longitudinal polarization fraction in a pure-penguin mode from $R_L \sim 0.9$ down to 0.75 [3]. Therefore, the $B^+ \rightarrow \rho^+ K^{*0}$ polarization data in Table 1 can be well accommodated within the Standard Model, showing no anomaly. The longitudinal polarization fraction of another mode $B^+ \rightarrow \rho^0 K^{*+}$ remains as $R_L \sim 0.9$ because of the interference between the penguin amplitude and an additional tree amplitude. From the viewpoint of PQCD, the $B \rightarrow \omega K^*$ decays do not differ much from $B \rightarrow \rho^0 K^*$, and are expected to show similar R_L . This prediction can be tested by the future data.

The fourth category, involving the $B \rightarrow \phi K^*$ decays, is the abnormal one. These decays occur mainly through the penguin operators, but their R_L are as small as 0.5, much lower than 0.75 expected from PQCD. The mechanism proposed in the literature to explain the $B \rightarrow \phi K^*$ polarization data includes new physics [13], the annihilation contribution [14] in the framework based on the QCD-improved factorization (QCDF) [15], the charming penguin [16], the rescattering effect [17, 18, 19], and the $b \rightarrow sg$ transition (the magnetic penguin) [20]. We shall comment on these proposals: the annihilation contribution has to be parameterized in QCDF, and varying free parameters to fit the data can not be conclusive. The charming penguin strategy, demanding many free parameters, does not help understand dynamics. The rescattering effect is based on a model-dependent analysis [21, 22], and constrained by the $B \rightarrow \rho K^*$ data. The magnetic penguin is suppressed by the G -parity, and not sufficient to reduce R_L down to 0.5. Therefore, none of these proposals is satisfactory [4]. However, we are not concluding that the $B \rightarrow \phi K^*$ polarization data signal new physics, since the complicated QCD dynamics in $B \rightarrow VV$ modes has not yet been fully explored.

In Sec. II we study the kinematic effects on the polarizations of tree-dominated decays using FA in the heavy-quark or large-energy limit. The next-to-leading-power corrections to the $B \rightarrow D_{(s)}^* D^*$ decays, and the two-parton twist-4 corrections to the $B \rightarrow \rho\rho$ decays are calculated in Sec. III. We comment on the proposals for explaining the abnormal $B \rightarrow \phi K^*$ data in Sec. IV. Section V is the conclusion.

2 NAIVE FACTORIZATION

In this section we demonstrate that the polarization fractions of tree-dominated $B \rightarrow VV$ decays can be simply understood by means of kinematics in the heavy-quark or large-energy limit.

2.1 Heavy-quark Limit

We first investigate the polarizations in the decays $B^0 \rightarrow (D_s^{*+}, D^{*+}, \rho^+) D^{*-}$ in the heavy quark limit. These modes are color-allowed with the D_s^{*+}, D^{*+}, ρ^+ mesons emitted from the weak vertex, respectively, and FA is supposed to work well. Take the $B^0 \rightarrow D_s^{*+} D^{*-}$ decay as an example. The B meson momentum P_1 , the D^* meson momentum P_2 , and the D_s^* meson momentum P_3 are chosen, in the light-cone coordinates, as

$$\begin{aligned} P_1 &= \frac{m_B}{\sqrt{2}}(1, 1, 0_T) , \\ P_2 &= \frac{m_B}{\sqrt{2}}(r_2\eta^+, r_2\eta^-, \mathbf{0}_T) , \\ P_3 &= \frac{m_B}{\sqrt{2}}(1 - r_2\eta^+, 1 - r_2\eta^-, \mathbf{0}_T) , \end{aligned} \quad (3)$$

where the factors η^\pm are defined by $\eta^\pm = \eta \pm \sqrt{\eta^2 - 1}$ with $\eta = v_1 \cdot v_2$ being the velocity transfer, $v_1 \equiv P_1/m_B$ and $v_2 \equiv P_2/m_{D^*}$ the B meson and D^* meson velocities, respectively, and $r_2 = m_{D^*}/m_B$ the mass ratio. To extract the helicity amplitudes, the following parametrization for the longitudinal polarization vectors is useful:

$$\begin{aligned} \epsilon_2(L) &= v_2 - \frac{m_{D^*}}{P_2 \cdot n_-} n_- = \frac{1}{\sqrt{2}}(\eta^+, -\eta^-, \mathbf{0}_T) , \\ \epsilon_3(L) &= v_3 - \frac{m_{D_s^*}}{P_3 \cdot n_+} n_+ = \frac{1}{\sqrt{2}r_3} \left(-\frac{r_3^2}{1 - r_2\eta^-}, 1 - r_2\eta^-, \mathbf{0}_T \right) , \end{aligned} \quad (4)$$

with the D_s^* meson velocity $v_3 \equiv P_3/m_{D_s^*}$, the mass ratio $r_3 = m_{D_s^*}/m_B$, and the null vectors $n_+ = (1, 0, \mathbf{0}_T)$ and $n_- = (0, 1, \mathbf{0}_T)$, which satisfy the normalization $\epsilon_2^2(L) = \epsilon_3^2(L) = -1$ and the orthogonality $\epsilon_2(L) \cdot P_2 = \epsilon_3(L) \cdot P_3 = 0$. For the transverse polarization vectors, we simply choose

$$\epsilon_2(T) = (0, 0, \mathbf{1}_T) , \quad \epsilon_3(T) = (0, 0, \mathbf{1}_T) . \quad (5)$$

The relevant effective weak Hamiltonian is given by

$$\mathcal{H}_{\text{eff}} = \frac{G_F}{\sqrt{2}} V_{cb} V_{cs}^* [C_1(\mu) O_1(\mu) + C_2(\mu) O_2(\mu)] , \quad (6)$$

where V 's are the Cabibbo-Kobayashi-Maskawa (CKM) matrix elements, C_1 and C_2 the Wilson coefficients, and

$$O_1 = (\bar{s}b)_{V-A}(\bar{c}c)_{V-A} , \quad O_2 = (\bar{c}b)_{V-A}(\bar{s}c)_{V-A} , \quad (7)$$

the four-fermion operators with the definition $(\bar{q}_1 q_2)_{V-A} \equiv \bar{q}_1 \gamma_\mu (1 - \gamma_5) q_2$. The contributions from O_1 and O_2 can be combined, and the resultant coefficient appears as $a_1 = C_2 + C_1/N_c$, N_c being the number of colors.

The $B^0 \rightarrow D_s^{*+} D^{*-}$ decay amplitude in FA is expressed as

$$\begin{aligned} \mathcal{M}^{(\sigma)} &= \langle D_s^{*+}(P_3, \epsilon_3^*) D^{*-}(P_2, \epsilon_2^*) | \mathcal{H}_{\text{eff}} | B^0(P_1) \rangle , \\ &= \frac{G_F}{\sqrt{2}} V_{cb}^* V_{cs} a_1 \langle D_s^{*+}(P_3, \epsilon_3^*) | \bar{c} \gamma_\mu (1 - \gamma_5) s | 0 \rangle \\ &\quad \times \langle D^{*-}(P_2, \epsilon_2^*) | \bar{b} \gamma^\mu (1 - \gamma_5) c | B^0(P_1) \rangle , \end{aligned} \quad (8)$$

where the superscript σ denotes a possible final helicity state. The first matrix element defines the D_s^* meson decay constant,

$$\langle D_s^{*+}(P_3, \epsilon_3^*) | \bar{c} \gamma_\mu (1 - \gamma_5) s | 0 \rangle = m_{D_s^*} f_{D_s^*} \epsilon_{3\mu}^* . \quad (9)$$

The matrix elements for the $B \rightarrow D^*$ transitions are parameterized as

$$\begin{aligned} \langle D^{*-}(P_2, \epsilon_2^*) | \bar{b} \gamma^\mu c | B^0(P_1) \rangle &= i \sqrt{m_B m_{D^*}} \xi_V(\eta) \epsilon^{\mu\nu\alpha\beta} \epsilon_{2\nu}^* v_{2\alpha} v_{1\beta} , \\ \langle D^{*-}(P_2, \epsilon_2^*) | \bar{b} \gamma^\mu \gamma_5 c | B^0(P_1) \rangle &= \sqrt{m_B m_{D^*}} [\xi_{A1}(\eta)(\eta + 1) \epsilon_2^{*\mu} - \xi_{A2}(\eta) \epsilon_2^* \cdot v_1 v_1^\mu \\ &\quad - \xi_{A3}(\eta) \epsilon_2^* \cdot v_1 v_2^\mu] , \end{aligned} \quad (10)$$

where the form factors ξ_{A1} , ξ_{A2} , ξ_{A3} , and ξ_V satisfy the relations in the heavy-quark limit,

$$\xi_V = \xi_{A1} = \xi_{A3} = \xi, \quad \xi_{A2} = 0 , \quad (11)$$

with ξ being the IW function [10].

The $B^0 \rightarrow D_s^{*+} D^{*-}$ decay rate is given by

$$\Gamma = \frac{P_c}{8\pi m_B^2} \sum_{\sigma} \mathcal{M}^{(\sigma)\dagger} \mathcal{M}^{(\sigma)} , \quad (12)$$

where $P_c \equiv |P_{2z}| = |P_{3z}| = m_B r_2 \sqrt{\eta^2 - 1}$ is the momentum of either of the vector mesons. The amplitude $\mathcal{M}^{(\sigma)}$ is decomposed into

$$\mathcal{M}^{(\sigma)} = \left(m_B^2 \mathcal{M}_L, m_B^2 \mathcal{M}_N \epsilon_2^*(T) \cdot \epsilon_3^*(T), i \mathcal{M}_T \epsilon^{\alpha\beta\gamma\rho} \epsilon_{2\alpha}^* \epsilon_{3\beta}^* P_{2\gamma} P_{3\rho} \right) , \quad (13)$$

where the first term corresponds to the configuration with both the vector mesons being longitudinally polarized, and the second (third) term to the two configurations with both the vector mesons being transversely polarized in the parallel (perpendicular) directions. The helicity amplitudes are then defined as,

$$\begin{aligned} A_L &= -G m_B^2 \mathcal{M}_L, \\ A_{\parallel} &= G \sqrt{2} m_B^2 \mathcal{M}_N, \\ A_{\perp} &= G m_{D_s^*} m_{D^*} \sqrt{2[(v_2 \cdot v_3)^2 - 1]} \mathcal{M}_T , \end{aligned} \quad (14)$$

with the normalization factor $G = \sqrt{P_c/(8\pi m_B^2 \Gamma)}$, which satisfy the relation,

$$|A_L|^2 + |A_{\parallel}|^2 + |A_{\perp}|^2 = 1. \quad (15)$$

It is easy to read the helicity amplitudes off Eqs. (8)-(10),

$$\begin{aligned} A_L &\propto \epsilon_2^*(L) \cdot \epsilon_3^*(L)(\eta + 1)\xi_{A_1} - \epsilon_2^*(L) \cdot v_1 [\epsilon_3^*(L) \cdot v_1 \xi_{A_2} + \epsilon_3^*(L) \cdot v_2 \xi_{A_3}] , \\ A_{\parallel} &\propto -\sqrt{2}(\eta + 1)\xi_{A_1} , \\ A_{\perp} &\propto -r_3 \sqrt{2[(v_2 \cdot v_3)^2 - 1]}\xi_V . \end{aligned} \quad (16)$$

In the heavy-quark limit, i.e., applying Eq. (11), all the helicity amplitudes depend on a single IW function ξ , which absorbs QCD dynamics. Simply inserting $m_B = 5.28$ GeV, $m_{D_s^*} = 2.11$ GeV, and $m_{D^*} = 2.01$ GeV into the kinematic factors, we obtain

$$R_L \sim 0.52, \quad R_{\parallel} \sim 0.43, \quad R_{\perp} \sim 0.05. \quad (17)$$

Equation (16) is applicable to the $B^0 \rightarrow D^{*+}D^{*-}$ and $B^0 \rightarrow \rho^+D^{*-}$ decays by substituting m_{D^*} and $m_{\rho} = 0.77$ GeV for $m_{D_s^*}$, leading to

$$R_L \sim 0.54, \quad R_{\parallel} \sim 0.41, \quad R_{\perp} \sim 0.05, \quad (18)$$

$$R_L \sim 0.88, \quad R_{\parallel} \sim 0.10, \quad R_{\perp} \sim 0.02, \quad (19)$$

respectively. All the above results are consistent with the observed values listed in Table 2, and with the predictions in [29]. The estimated polarization fractions for the decay $B^- \rightarrow K^{*-}D^{*0}$ are close to Eq. (19) and consistent with the data. For the $B^+ \rightarrow \rho^+\bar{D}^{*0}$ decay, the internal- W emission amplitudes involving the $B \rightarrow \rho$ form factors are suppressed by the vanishing coefficient $a_2 = C_1 + C_2/N_c$. Hence, this mode is similar to $B^0 \rightarrow \rho^+D^{*-}$, and the result in Eq. (19) applies as shown in Table 2. It is easy to find that the longitudinal polarization fraction increases as the mass of the vector meson from the weak vertex decreases.

2.2 Large-energy Limit

We then show that the polarization fractions in the $B \rightarrow (\rho, \omega)\rho$ decays can be understood by means of kinematics in the large-energy limit. The parametrizations of the momenta in Eq. (3) and of the polarization vectors in Eqs. (4) and (5) hold here, with the mass ratio r_2 for the vector meson from the B meson transition and r_3 for the vector meson emitted from the weak vertex. The transition form factors associated with a $B \rightarrow V$ transition are defined via the matrix elements,

$$\langle V(P_2, \epsilon_2^*) | \bar{b}\gamma^\mu q | B(P_1) \rangle = \frac{2iV(q^2)}{m_B + m_V} \epsilon^{\mu\nu\rho\sigma} \epsilon_{2\nu}^* P_{2\rho} P_{1\sigma}, \quad (20)$$

$$\begin{aligned} \langle V(P_2, \epsilon_2^*) | \bar{b}\gamma^\mu \gamma_5 q | B(P_1) \rangle &= 2m_V A_0(q^2) \frac{\epsilon_2^* \cdot q}{q^2} q^\mu + (m_B + m_V) A_1(q^2) \left(\epsilon_2^{*\mu} - \frac{\epsilon_2^* \cdot q}{q^2} q^\mu \right) \\ &\quad - A_2(q^2) \frac{\epsilon_2^* \cdot q}{m_B + m_V} \left(P_1^\mu + P_2^\mu - \frac{m_B^2 - m_V^2}{q^2} q^\mu \right), \end{aligned} \quad (21)$$

Mode	Pol. Fraction	Data	
$B^0 \rightarrow D_s^{*+} D^{*-}$	R_L	0.52 ± 0.05 [23]	
$B^0 \rightarrow D^{*+} D^{*-}$	R_L	$0.57 \pm 0.08 \pm 0.02$ [24]	
	R_\perp	$0.19 \pm 0.08 \pm 0.01$ [24]	
	R_\perp	$0.063 \pm 0.055 \pm 0.009$ [23, 25]	
$B^0 \rightarrow \rho^+ D^{*-}$	R_L	$0.885 \pm 0.016 \pm 0.012$ [23]	
$B^+ \rightarrow \rho^+ \bar{D}^{*0}$	R_L	$0.892 \pm 0.018 \pm 0.016$ [23]	
$B^- \rightarrow K^{*-} D^{*0}$	R_L	$0.86 \pm 0.06 \pm 0.03$ [26]	
Mode	Pol. Fraction	Belle	Babar
$B^+ \rightarrow \rho^+ \rho^0$	R_L	$0.95 \pm 0.11 \pm 0.02$ [1]	$0.97^{+0.03}_{-0.07} \pm 0.04$ [2]
$B^0 \rightarrow \rho^+ \rho^-$	R_L		$0.99 \pm 0.03^{+0.04}_{-0.03}$ [27]
$B^+ \rightarrow \rho^+ \omega$	R_L		$0.88^{+0.12}_{-0.15} \pm 0.03$ [28]

Table 2: Polarization fractions in the tree-dominated $B \rightarrow VV$ decays.

with the momentum $q = P_1 - P_2$. The form factors V , A_1 , and A_2 satisfy the symmetry relations in the large-energy limit,

$$\frac{m_B}{m_B + m_V} V(q^2) = \frac{m_B + m_V}{2E} A_1(q^2) = \xi_\perp(E) , \quad (22)$$

$$\frac{m_B + m_V}{2E} A_1(q^2) - \frac{m_B - m_V}{m_B} A_2(q^2) = \frac{m_V}{E} \xi_\parallel(E) , \quad (23)$$

where E is the V meson energy, and the function $\xi_\parallel(E)$ ($\xi_\perp(E)$) is associated with the transition into a longitudinally (transversely) polarized V meson. Our definition of ξ_\parallel differs from those in [30, 31], such that we have $\xi_\perp \approx \xi_\parallel$, when not distinguishing the longitudinal and transverse polarizations.

Consider the $B^+ \rightarrow \rho^+ \rho^0$ mode as an example, which is dominated by a tree contribution (assuming that the electroweak penguin contribution is negligible). The explicit expression of the relevant effective weak Hamiltonian will not be shown here. In FA, the decay amplitude is written as

$$\begin{aligned} \langle \rho^+ \rho^0 | \mathcal{H}_{\text{eff}} | B^+ \rangle &= \frac{G_F}{\sqrt{2}} V_{ub}^* V_{ud} \left[a_1 \langle \rho^+(P_3, \epsilon_3^*) | \bar{u} \gamma_\mu (1 - \gamma_5) d | 0 \rangle \langle \rho^0(P_2, \epsilon_2^*) | \bar{b} \gamma^\mu (1 - \gamma_5) u | B^+(P_1) \rangle \right. \\ &\quad \left. + a_2 \langle \rho^0(P_2, \epsilon_2^*) | \bar{u} \gamma_\mu (1 - \gamma_5) u | 0 \rangle \langle \rho^+(P_3, \epsilon_3^*) | \bar{b} \gamma^\mu (1 - \gamma_5) d | B^+(P_1) \rangle \right] , \end{aligned} \quad (24)$$

where the two terms can be combined, leading to the helicity amplitudes,

$$\begin{aligned} A_L &\propto (1 + r_2) \epsilon_2^*(L) \cdot \epsilon_3^*(L) \left[A_1 - \frac{2\epsilon_2^* \cdot P_3 P_2 \cdot \epsilon_3^*}{m_B^2 (1 + r_2)^2 \epsilon_2^* \cdot \epsilon_3^*} A_2 \right] , \\ A_\parallel &\propto -\sqrt{2} (1 + r_2) A_1 , \\ A_\perp &\propto -\frac{2r_2 r_3}{1 + r_2} \sqrt{2[(v_2 \cdot v_3)^2 - 1]} V . \end{aligned} \quad (25)$$

The relative phases among the helicity amplitudes are $\phi_{\parallel} = \phi_{\perp} = \pi$ under FA in our convention. In the large-energy limit, i.e., employing Eqs. (22) and (23), Eq. (25) becomes

$$\begin{aligned} A_L &\propto 2r_2\epsilon_2^*(L) \cdot \epsilon_3^*(L)\xi_{\parallel} , \\ A_{\parallel} &\propto -2\sqrt{2}r_2\eta\xi_{\perp} , \\ A_{\perp} &\propto -2r_2r_3\sqrt{2[(v_2 \cdot v_3)^2 - 1]}\xi_{\perp} , \end{aligned} \quad (26)$$

implying that QCD dynamics has been absorbed into the two functions ξ_{\parallel} and ξ_{\perp} . For a rough estimate, adopting $\xi_{\parallel} \approx (f_{\rho}/f_{\rho}^T)\xi_{\perp}$, $f_{\rho} = 200$ MeV and $f_{\rho}^T = 160$ MeV [32], the $B^+ \rightarrow \rho^+\rho^0$ polarization fractions are given by,

$$R_L \sim 0.95 , \quad R_{\parallel} \sim 0.03 , \quad R_{\perp} \sim 0.02 , \quad (27)$$

consistent with the data in Table 2. The polarization fractions of other tree-dominated $B \rightarrow VV$ modes, including $\rho^+\rho^-$ and $\rho^+\omega$, can be explained in a similar way.

We generalize Eq. (26) to the $B^+ \rightarrow (D_s^{*+}, D^{*+})\rho^0$ modes, which are mainly governed by the $B \rightarrow \rho$ form factors, with the masses $m_{D_s^*}$, m_{D^*} being substituted for m_{ρ} , respectively. Their polarization fractions are predicted to be,

$$\begin{aligned} D_s^{*+}\rho^0 : \quad & R_L \sim 0.70 , \quad R_{\parallel} \sim 0.16 , \quad R_{\perp} \sim 0.14 , \\ D^{*+}\rho^0 : \quad & R_L \sim 0.72 , \quad R_{\parallel} \sim 0.15 , \quad R_{\perp} \sim 0.13 , \end{aligned} \quad (28)$$

which can be compared with the data in the future.

3 SUBLEADING CORRECTIONS

Away from the heavy quark limit, the form factors in Eq. (10) deviate from the IW function. Beyond FA, nonfactorizable contributions appear. Both corrections, being subleading [33, 34], can be calculated more reliably in the PQCD approach based on k_T factorization theorem [35, 36] due to the stronger end-point suppression in the former [33] and to the soft cancellation between a pair of nonfactorizable diagrams in the latter [37]. In this section we shall examine whether the simple estimates made in the previous section are robust under these subleading corrections. The k_T factorization theorem for the $B \rightarrow D^*$ form factors in the large-recoil region of the D^* meson can be proved following the procedure in [38], which are expressed as the convolution of hard kernels with the B and D^* meson wave functions in both the momentum fractions x and the transverse momenta k_T of partons. A hard kernel, being infrared-finite, is calculable in perturbation theory. The B and D^* meson wave functions, collecting the soft dynamics in the decays, are not calculable but universal. After including the parton k_T , the end-point singularities, which usually break QCDF at subleading level, do not appear, and PQCD factorization formulas are well-defined. This formalism has been applied to the semileptonic decay $B \rightarrow D^{(*)}l\nu$ [33], and the nonleptonic decays $B \rightarrow D^{(*)}\pi(\rho)$ [34, 39] and $B \rightarrow D_s^{(*)}D_s^{(*)}$ [40] successfully.

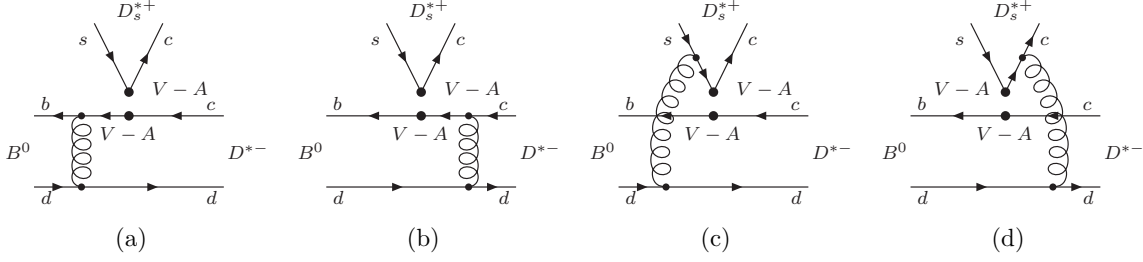


Figure 1: Lowest-order diagrams for the $B^0 \rightarrow D_s^{*+} D^{*-}$ decay.

3.1 $B^0 \rightarrow D_s^{*+} D^{*-}$

For the $B^0 \rightarrow D_s^{*+} D^{*-}$ mode, we shall neglect the penguin contribution, which is suppressed by the Wilson coefficients $C_{3-6} \sim 0.05a_1$. According to the lowest-order external- W emission diagrams in Fig. 1, the decay amplitudes for different final helicity states are expressed as

$$\begin{aligned} \mathcal{M}^{(\sigma)} = & \frac{G_F}{\sqrt{2}} V_{cb} V_{cs} \left[m_B^2 (f_{D_s^*} \mathcal{F}_L + \mathcal{M}_L), m_B^2 \epsilon_2^*(T) \cdot \epsilon_3^*(T) (f_{D_s^*} \mathcal{F}_N + \mathcal{M}_N), \right. \\ & \left. i \epsilon^{\alpha\beta\gamma\rho} \epsilon_{2\alpha}^* \epsilon_{3\beta}^* P_{2\gamma} P_{3\rho} (f_{D_s^*} \mathcal{F}_T + \mathcal{M}_T) \right], \end{aligned} \quad (29)$$

where $\mathcal{F}_{L,N,T}$ come from the factorizable diagrams, Figs. 1(a) and 1(b), and $\mathcal{M}_{L,N,T}$ from the nonfactorizable diagrams, Figs. 1(c) and 1(d).

We first compute each factorizable amplitude in terms of the “form factors” as an expansion in r_2 ,

$$\begin{aligned} \xi_i &= \xi + \xi_i^{(\text{NL})}, \quad i = A_1, A_3, V, \\ \xi_{A2} &= \xi_{A2}^{(\text{NL})}, \end{aligned} \quad (30)$$

where the superscript NL denotes the next-to-leading-power corrections. Equation (30) is equivalent to the heavy-quark expansion of the heavy-heavy currents in $1/m_b$ and in $1/m_c$ [41], m_b (m_c) being the b (c) quark mass. We refer the explicit expressions of the PQCD factorization formulas for ξ and $\xi_i^{(\text{NL})}$ to [33], which have absorbed the Wilson coefficient a_1 in the current analysis. In terms of Eq. (30), the factorizable amplitudes are written as

$$\begin{aligned} \mathcal{F}_L &= \sqrt{r_2} r_3 \left\{ \epsilon_2^*(L) \cdot \epsilon_3^*(L) (\eta + 1) \left(\xi + \xi_{A1}^{(\text{NL})} \right) \right. \\ &\quad \left. - \epsilon_2^*(L) \cdot v_1 \left[\epsilon_3^*(L) \cdot v_1 \xi_{A2}^{(\text{NL})} + \epsilon_3^*(L) \cdot v_2 \left(\xi + \xi_{A3}^{(\text{NL})} \right) \right] \right\}, \\ \mathcal{F}_N &= \sqrt{r_2} r_3 (\eta + 1) \left(\xi + \xi_{A1}^{(\text{NL})} \right), \\ \mathcal{F}_T &= \frac{r_3}{\sqrt{r_2}} \left(\xi + \xi_V^{(\text{NL})} \right). \end{aligned} \quad (31)$$

A numerical analysis gives

$$\xi_{A1}^{(\text{NL})} \sim -0.02 \xi, \quad \xi_{A2}^{(\text{NL})} \sim -0.19 \xi, \quad \xi_{A3,V}^{(\text{NL})} \sim -0.05 \xi. \quad (32)$$

Inserting the deviation from the IW function into Eq. (16), the polarization fractions are modified only slightly:

$$R_L \sim 0.54, \quad R_{\parallel} \sim 0.41, \quad R_{\perp} \sim 0.05. \quad (33)$$

The largest next-to-leading-power correction comes from $\xi_{A_2}^{(\text{NL})}$, which is, however, suppressed by the factor r_2 .

Next we calculate the subleading corrections from the nonfactorizable diagrams in Figs. 1(c) and 1(d). For simplicity, we shall expand all the kinematical factors and the polarization amplitudes up to next-to-leading power in $r_{2,3}$. The factorization formulas are given by

$$\begin{aligned} \mathcal{M}_L &= 16\pi C_F \sqrt{2N_c} m_B^2 \int_0^1 dx_1 dx_2 dx_3 \int_0^\infty b_1 db_1 b_3 db_3 \phi_B(x_1, b_1) \phi_{D^*}(x_2) \phi_{D_s^*}(x_3) \\ &\quad \times \left[(x_3 - x_1 + r_2 x_2) E_b(t_b^{(1)}) h_b^{(1)}(x_1, x_2, x_3, b_1, b_3) \right. \\ &\quad \left. - (1 + x_2 - x_3 - x_1 - x_2 r_2) E_b(t_b^{(2)}) h_b^{(2)}(x_1, x_2, x_3, b_1, b_3) \right], \end{aligned} \quad (34)$$

$$\begin{aligned} \mathcal{M}_N &= 16\pi C_F \sqrt{2N_c} m_B^2 \int_0^1 dx_1 dx_2 dx_3 \int_0^\infty b_1 db_1 b_3 db_3 \phi_B(x_1, b_1) \phi_{D^*}(x_2) \phi_{D_s^*}(x_3) \\ &\quad \times \left[x_3 r_3 E_b(t_b^{(1)}) h_b^{(1)}(x_1, x_2, x_3, b_1, b_3) \right. \\ &\quad \left. - (1 + x_3) r_3 E_b(t_b^{(2)}) h_b^{(2)}(x_1, x_2, x_3, b_1, b_3) \right], \end{aligned} \quad (35)$$

$$\mathcal{M}_T = 2\mathcal{M}_N. \quad (36)$$

Radiative corrections to the meson wave functions generate the double logarithms $\alpha_s \ln^2 k_T$ from the overlap of collinear and soft enhancements, whose Sudakov resummation has been studied in [42]. The Sudakov factors from k_T resummation for the B meson, the D^* meson and the D_s^* meson are given, according to [43], by

$$\begin{aligned} \exp[-S_B(\mu)] &= \exp \left[-s(k_1^-, b_1) - \frac{5}{3} \int_{1/b_1}^\mu \frac{d\bar{\mu}}{\bar{\mu}} \gamma(\alpha_s(\bar{\mu})) \right], \\ \exp[-S_{D^*}(\mu)] &= \exp \left[-s(k_2^+, b_2) - \frac{5}{3} \int_{1/b_2}^\mu \frac{d\bar{\mu}}{\bar{\mu}} \gamma(\alpha_s(\bar{\mu})) \right], \\ \exp[-S_{D_s^*}(\mu)] &= \exp \left[-s(k_3^-, b_3) - \frac{5}{3} \int_{1/b_3}^\mu \frac{d\bar{\mu}}{\bar{\mu}} \gamma(\alpha_s(\bar{\mu})) \right], \end{aligned} \quad (37)$$

respectively, with the quark anomalous dimension $\gamma = -\alpha_s/\pi$. The momenta $k_1^- = x_1 P_1^-$, $k_2^+ = x_2 P_2^+$, and $k_3^- = x_3 P_3^-$, carried by the light valence quarks in the B , D^* , and D_s^* mesons, respectively, define the momentum fractions x . The impact parameters b_1 , b_2 , and b_3 are conjugate to the transverse momenta carried by the light valence quarks in the B , D^* , and D_s^* mesons, respectively. For the explicit expression of the Sudakov exponent s , refer to [11]. Note that the coefficient $5/3$ of the quark anomalous dimension in Eq. (37) differs from 2 for a light meson. The reason is that the rescaled heavy-quark field adopted in the definition of a heavy-meson wave function has a self-energy correction different from that of the full heavy-quark field [43]. The evolution factors are then given by

$$E_b(t) = \alpha_s(t) \frac{C_1(t)}{N_c} \exp[-S(t)|_{b_2=b_1}], \quad (38)$$

with the Sudakov exponent $S = S_B + S_{D^*} + S_{D_s^*}$.

The functions $h_b^{(j)}$, $j = 1$ and 2 , are written as

$$\begin{aligned} h_b^{(j)} &= [\theta(b_1 - b_3) K_0(Bm_B b_1) I_0(Bm_B b_3) \\ &\quad + \theta(b_3 - b_1) K_0(Bm_B b_3) I_0(Bm_B b_1)] \\ &\quad \times \begin{pmatrix} K_0(B_j m_B b_3) & \text{for } B_j^2 \geq 0 \\ \frac{i\pi}{2} H_0^{(1)}(\sqrt{|B_j^2|} m_B b_3) & \text{for } B_j^2 \leq 0 \end{pmatrix}, \end{aligned} \quad (39)$$

with the variables

$$\begin{aligned} B^2 &= x_1 x_2 r_2 \eta^+, \\ B_1^2 &= x_1 x_2 r_2 \eta^+ - x_2 x_3 (r_2 \eta^+ - r_2^2), \\ B_2^2 &= x_1 x_2 r_2 \eta^+ - x_2 (1 - x_3) (r_2 \eta^+ - r_2^2) + (x_1 + x_3) (1 - r_2 \eta^+) + x_3 (r_2^2 - r_2 \eta^-). \end{aligned} \quad (40)$$

The scales $t_b^{(j)}$ are chosen as

$$t_b^{(j)} = \max(Bm_B, \sqrt{|B_j^2|} m_B, 1/b_1, 1/b_3). \quad (41)$$

The B and D^* meson wave functions involved in Eqs. (34)-(36) are also referred to [33]:

$$\phi_B(x, b) = N_B x^2 (1 - x)^2 \exp \left[-\frac{1}{2} \left(\frac{x m_B}{\omega_B} \right)^2 - \frac{\omega_B^2 b^2}{2} \right], \quad (42)$$

$$\phi_{D^*}(x) = \frac{3f_{D^*}}{\sqrt{2N_c}} x(1 - x) [1 + C_{D^*}(1 - 2x)]. \quad (43)$$

The D_s^* meson wave function $\phi_{D_s^*}$ will be assumed to have the same functional form as ϕ_{D^*} . We do not consider the b dependence of ϕ_{D^*} in the large recoil region of the D^* meson [33]. The Gaussian form of ϕ_B was motivated by the oscillator model in [44]. The shape parameter $\omega_B = 0.40$ GeV comes from [45], and $C_{D^*} = 1.04$ is determined from the IW function $\xi(\eta = 1.3) = 0.7$. The normalization constant N_B is related to the decay constant f_B through

$$\int dx \phi_B(x, b = 0) = \frac{f_B}{2\sqrt{2N_c}}. \quad (44)$$

We shall not distinguish the D^* meson wave functions associated with the longitudinal and transverse polarizations. There are various models of the B meson wave functions available in the literature [43]. It has been confirmed that the model in Eq. (42) and the model derived in [46] with a different functional form lead to similar numerical results for the $B \rightarrow \pi$ form factor [47].

Taking into account only the nonfactorizable corrections, the polarization fractions become

$$R_L \sim 0.54, \quad R_{\parallel} \sim 0.40, \quad R_{\perp} \sim 0.06. \quad (45)$$

Including both the subleading factorizable and nonfactorizable corrections, we have

$$R_L \sim 0.56, \quad R_{\parallel} \sim 0.39, \quad R_{\perp} \sim 0.06, \quad (46)$$

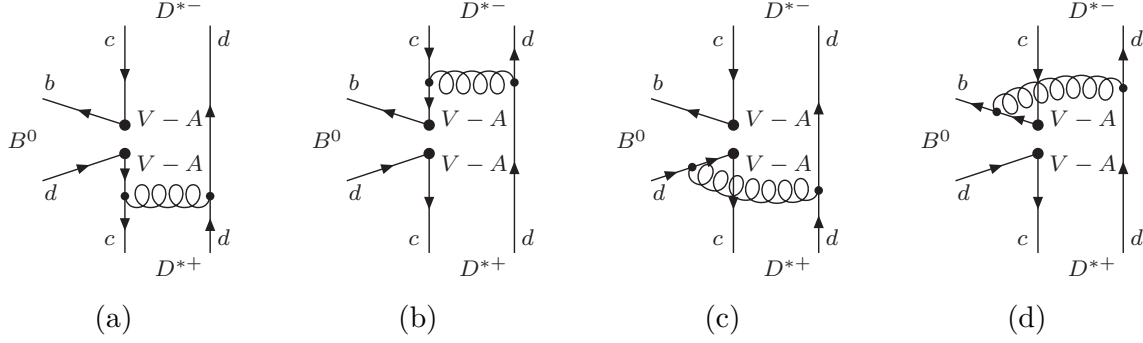


Figure 2: W -exchange diagrams for the $B^0 \rightarrow D^{*+} D^{*-}$ decay.

which are still close to the values in Eq. (17). Hence, the simple kinematic estimate made in the heavy-quark limit is very reliable.

At last, we compute the $B^0 \rightarrow D_s^{*+} D^{*-}$ branching ratio, considering only the leading contribution. Employing the CKM matrix elements $V_{cb} = 0.0412$, $V_{cs} = 0.996$, and $V_{cd} = -0.224$, the quark masses $m_b = 4.8$ GeV and $m_t = 174.3$ GeV, the meson decay constants $f_B = 200$ MeV, $f_{D^*} = 230$ MeV, and $f_{D_s^*} = 240$ MeV, the lifetimes $\tau_{B^0} = 1.542 \times 10^{-12}$ sec and $\tau_{B^\pm} = 1.674 \times 10^{-12}$ sec, and the Fermi constant $G_F = 1.16639 \times 10^{-5}$ GeV $^{-2}$, we predict

$$B(B^0 \rightarrow D_s^{*+} D^{*-}) = (2.6_{-0.8}^{+1.1})\%, \quad (47)$$

which is consistent with the recent measurement $(1.85 \pm 0.09 \pm 0.16)\%$ [48]. The theoretical uncertainty in Eq. (47) arises from the allowed range of the shape parameter $\omega_B = (0.40 \pm 0.04)$ GeV [45] in the B meson wave function. Note that the polarization fractions are insensitive to this overall source of uncertainty.

3.2 $B \rightarrow D^* D^*$

For the $B^0 \rightarrow D^{*+} D^{*-}$ mode, there exists an additional contribution from the W -exchange topology shown in Fig. 2 compared to $B^0 \rightarrow D_s^{*+} D^{*-}$. The factorizable W -exchange diagrams, Figs. 2(a) and 2(b), vanish exactly because of the helicity suppression. An explicit evaluation shows that the nonfactorizable W -exchange diagrams, Figs. 2(c) and 2(d), contribute only 2% of the external- W emission ones in Fig. 1. Therefore, the W -exchange topology is even less important than the penguin one. Note that the W -exchange contribution is as important as the nonfactorizable contribution for the $B \rightarrow D^{(*)} \pi(\rho)$ decays [34], to which the helicity suppression does not apply. The $B^0 \rightarrow D^{*+} D^{*-}$ factorization formulas are then similar to those of $B^0 \rightarrow D_s^{*+} D^{*-}$ but with the appropriate replacements of the D_s^* meson mass, decay constant, and wave function by the D^* meson ones, respectively. Similarly, if neglecting the W -exchange and penguin contributions, the $B^+ \rightarrow D^{*+} \bar{D}^{*0}$ decay amplitudes will be the same as of $B^0 \rightarrow D^{*+} D^{*-}$.

The numerical results are summarized below. Including both the subleading factorizable and nonfactorizable corrections, we obtain the polarization fractions of the $B^0 \rightarrow D^{*+} D^{*-}$ and $B^+ \rightarrow D^{*+} \bar{D}^{*0}$ modes,

$$R_L \sim 0.56, \quad R_{\parallel} \sim 0.38, \quad R_{\perp} \sim 0.06, \quad (48)$$

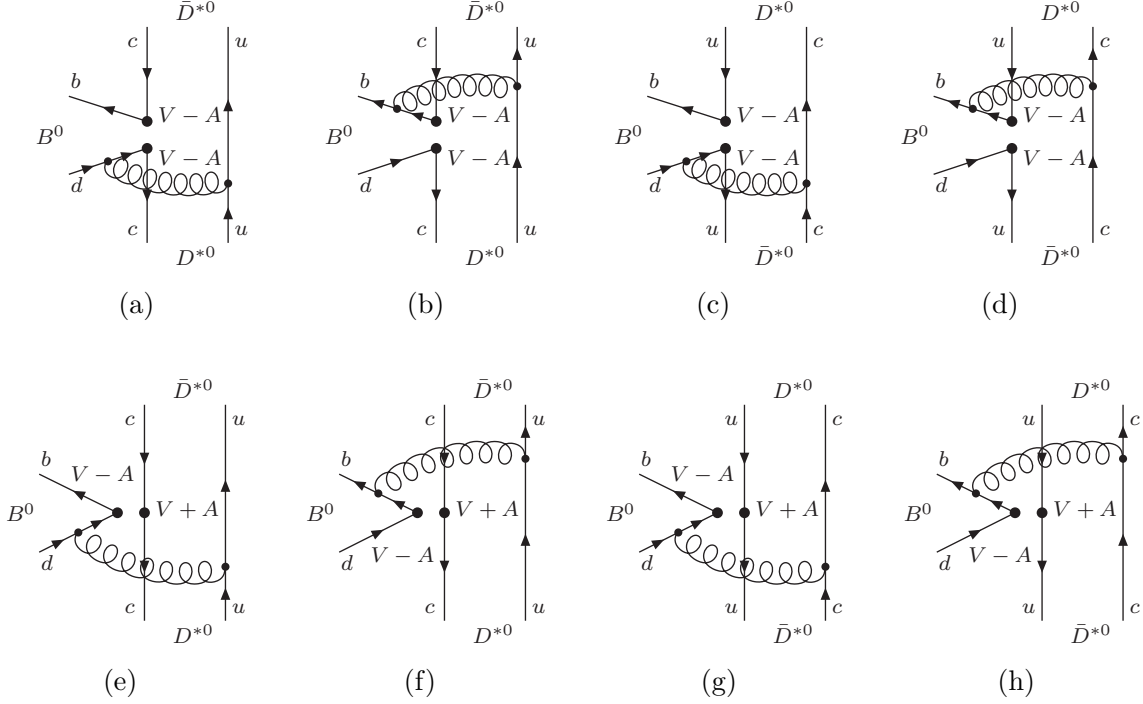


Figure 3: Lowest-order diagrams for the $B^0 \rightarrow \bar{D}^{*0} D^{*0}$ decay.

which are also close to the simple estimate in Eq. (18). Using the same input parameters for the quark masses, the B meson lifetimes,..., we predict the branching ratio,

$$B(B^0 \rightarrow D^{*+} D^{*-}) = \left(1.2^{+0.5}_{-0.3}\right) \times 10^{-3}, \quad (49)$$

which is consistent with the updated measurement $B(B^0 \rightarrow D^{*+} D^{*-}) = (8.1 \pm 0.8 \pm 0.1) \times 10^{-4}$ [24]. The branching ratio $B(B^+ \rightarrow D^{*+} D^{*0})$ can be obtained simply by changing the B meson lifetime, whose value is close to that in Eq. (49).

Since only the W -exchange topology in Figs. 3(a)-(d) and the penguin annihilation topology in Figs. 3(e)-(h) contribute, the $B^0 \rightarrow \bar{D}^{*0} D^{*0}$ decay must have a tiny branching ratio. For both topologies, the factorizable amplitudes diminish because of the helicity suppression (only the penguin annihilation from the $(S - P)(S + P)$ operators survives, which do not exist in this mode). Hence, they are not exhibited in Fig. 3. With the penguin amplitudes being down by the Wilson coefficients, we shall calculate only the tree contribution. By measuring the $B^0 \rightarrow \bar{D}^{*0} D^{*0}$ mode, we learn how the nonfactorizable W -exchange contribution governs the polarization fractions. It will be shown that the polarization fractions in this decay differ dramatically from those in the $B^0 \rightarrow D^{*+} D^{*-}$ and $B^+ \rightarrow D^{*+} \bar{D}^{*0}$ decays. On the other hand, it has been proposed [49] to extract the weak phase ϕ_3 from the $B \rightarrow D^{(*)} D^{(*)}$, $D_s^{(*)} D^{(*)}$ measurements.

The amplitudes from Figs. 3(a) and 3(b) are given by

$$\begin{aligned} \mathcal{M}_L = & 16\pi C_F \sqrt{2N_c} m_B^2 \int_0^1 dx_1 dx_2 dx_3 \int_0^\infty b_1 db_1 b_2 db_2 \phi_B(x_1, b_1) \phi_{D^*}(x_2) \phi_{D^*}(x_3) \\ & \times \left[(x_3 - x_1) E_f(t_f^{(1)}) h_f^{(1)}(x_1, x_2, x_3, b_1, b_2) \right] \end{aligned}$$

$$-x_2 E_f(t_f^{(2)}) h_f^{(2)}(x_1, x_2, x_3, b_1, b_2) \Big] , \quad (50)$$

$$\mathcal{M}_{N,T} = O(r_i^2) , \quad (51)$$

and those from Figs. 3(c) and 3(d) are

$$\begin{aligned} \mathcal{M}'_L = & 16\pi C_F \sqrt{2N_c} m_B^2 \int_0^1 dx_1 dx_2 dx_3 \int_0^\infty b_1 db_1 b_2 db_2 \phi_B(x_1, b_1) \phi_{D^*}(x_2) \phi_{D^*}(x_3) \\ & \times \left[(1-x_2) E_f(t_f'^{(1)}) h_f'^{(1)}(x_1, x_2, x_3, b_1, b_2) \right. \\ & \left. - (1-x_3+x_1) E_f(t_f'^{(2)}) h_f'^{(2)}(x_1, x_2, x_3, b_1, b_2) \right] , \end{aligned} \quad (52)$$

$$\mathcal{M}'_{N,T} = O(r_i^2) . \quad (53)$$

It is observed that the transverse polarization amplitudes vanish in the current next-to-leading-power accuracy. The evolution factors are

$$E_f(t) = \alpha_s(t) \frac{C_2(t)}{N_c} \exp[-S(t)|_{b_3=b_2}] . \quad (54)$$

The hard functions $h_f^{(j)}$, $j = 1$ and 2 , are written as

$$\begin{aligned} h_f^{(j)} = & \frac{i\pi}{2} \left[\theta(b_1 - b_2) H_0^{(1)}(F^{(j)} m_B b_1) J_0(F^{(j)} m_B b_2) \right. \\ & \left. + \theta(b_2 - b_1) H_0^{(1)}(F^{(j)} m_B b_2) J_0(F^{(j)} m_B b_1) \right] \\ & \times \left(\begin{array}{ll} K_0(F_j^{(j)} m_B b_1) & \text{for } F_j^{(j)2} \geq 0 \\ \frac{i\pi}{2} H_0^{(1)}(\sqrt{|F_j^{(j)2}|} m_B b_1) & \text{for } F_j^{(j)2} \leq 0 \end{array} \right) , \end{aligned} \quad (55)$$

with the variables

$$\begin{aligned} F^2 &= x_2 r_2 \eta^+ x_3 (1 - r_2 \eta^-) , \\ F_1^2 &= x_2 r_2 \eta^+ [x_1 - x_3 (1 - r_2 \eta^-)] , \\ F_2^2 &= 1 + (1 - x_2 r_2 \eta^+) [x_1 - 1 + x_3 (1 - r_2 \eta^-)] , \\ F'^2 &= (1 - x_2 r_2 \eta^+) [1 - x_3 (1 - r_2 \eta^-)] , \\ F_1'^2 &= (1 - x_2 r_2 \eta^+) [x_1 - 1 + x_3 (1 - r_2 \eta^-)] , \\ F_2'^2 &= 1 + x_2 r_2 \eta^+ [x_1 - x_3 (1 - r_2 \eta^-)] . \end{aligned} \quad (56)$$

The variables F' 's can be obtained from F 's by interchanging $x_2 r_2 \eta^+$ and $1 - x_2 r_2 \eta^+$, and $x_3 (1 - r_2 \eta^-)$ and $1 - x_3 (1 - r_2 \eta^-)$. The hard scales $t_f^{(j)}$ are chosen as

$$t_f^{(j)} = \max \left(F^{(j)} m_B, \sqrt{|F_j^{(j)2}|} m_B, 1/b_1, 1/b_2 \right) . \quad (57)$$

The longitudinal polarization fraction dominates:

$$R_L \sim 1, \quad R_{\parallel} \sim R_{\perp} \sim \text{few}\%, \quad (58)$$

which differs very much from that in Eq. (48). Therefore, the comparison of the theoretical prediction with the future data can test the PQCD approach. We also predict the branching ratio,

$$B(B^0 \rightarrow \bar{D}^{*0} D^{*0}) = (8.9_{-1.1}^{+1.4}) \times 10^{-5}, \quad (59)$$

which can also be compared with the future data.

3.3 $B \rightarrow \rho\rho$

In this subsection we examine whether the simple estimate of the polarization fractions in the tree-dominated B meson decays into two light vector mesons is robust under subleading corrections. Similar to the previous subsection, the $O(m_V/m_B)$ terms should be included into the factorizable amplitudes at this level of accuracy. At the same time, the two-parton twist-4 contribution appears, since the linear end-point singularity involved in collinear factorization theorem modifies the power behavior from $O(m_V^2/m_B^2)$ into $O(m_V/m_B)$ [45]. The inclusion of these two corrections makes complete the next-to-leading-power analysis at the two-parton level. The nonfactorizable amplitudes have been known to be small due to the strong cancellation between a pair of nonfactorizable diagrams [11, 12]. The annihilation amplitudes for tree-dominated modes are also negligible due to helicity suppression [37]. Hence, we shall not consider the two-parton twist-4 correction to these two subleading contributions. Below we analyze the $B \rightarrow \rho\rho$ longitudinal polarization amplitude as an example.

The two-parton ρ meson distribution amplitudes up to twist 4 are defined by the following expansion [32],

$$\begin{aligned} \langle \rho^-(P_2, \epsilon_{2L}^*) | \bar{d}(z)_j u(0)_l | 0 \rangle = & \frac{1}{\sqrt{2N_c}} \int_0^1 dx e^{ixp_2 \cdot z} \left[\not{p}_2 \phi_\rho(x) + m_\rho (\not{n}_+ \not{n}_- - 1) \phi_\rho^t(x) \right. \\ & \left. + m_\rho I \phi_\rho^s(x) - \frac{m_\rho^2}{2p_2 \cdot n_-} \not{n}_- \phi_\rho^g(x) \right]_{lj}, \end{aligned} \quad (60)$$

where the new vector p_2 contains only the plus (large) component of P_2 . The distribution amplitude ϕ_ρ is of twist 2 (leading twist), ϕ_ρ^t and ϕ_ρ^s of twist 3, and ϕ_ρ^g of twist 4. The twist-3 distribution amplitudes in fact give leading-power contribution due to the similar modification from the end-point singularity. The explicit expressions of the above ρ meson distribution amplitudes are referred to [45], and ϕ_ρ^g is given by [50]

$$\phi_\rho^g(x) = \frac{f_\rho}{2\sqrt{2N_c}} \left[1 - 1.62 C_2^{1/2}(2x-1) - 0.41 C_4^{1/2}(2x-1) \right], \quad (61)$$

with the Gegenbauer polynomials,

$$C_2^{1/2}(t) = \frac{1}{2}(3t^2 - 1), \quad C_4^{1/2}(t) = \frac{1}{8}(35t^4 - 30t^2 + 3). \quad (62)$$

The longitudinal factorizable amplitude in the $B \rightarrow \rho\rho$ decays is written, up to twist 4, as,

$$\begin{aligned} \mathcal{F}_L = & 8\pi C_F m_B^2 \int_0^1 dx_1 dx_2 \int_0^\infty b_1 db_1 b_2 db_2 \phi_B(x_1, b_1) \\ & \times \left\{ \left[\left((1+x_2)(1-r_2^2) - (1+2x_2)r_2^2 \right) \phi_\rho(x_2) \right. \right. \\ & \quad \left. \left. + r_2(1-2x_2) \left(\phi_\rho^s(x_2) + \phi_\rho^t(x_2) \right) \right] E_e(t_e^{(1)}) h_e(x_1, x_2, b_1, b_2) \right. \\ & \quad \left. + r_2 \left[2\phi_\rho^s(x_2) + r_2\phi_\rho^g(x_2) \right] E_e(t_e^{(2)}) h_e(x_2, x_1, b_2, b_1) \right\}, \end{aligned} \quad (63)$$

where the first (second) term containing $E_e(t_e^{(1)})$ [$E_e(t_e^{(2)})$] comes from the lowest-order diagram similar to Fig. 1(a) [Fig. 1(b)], but with the D_s^* and D^* mesons being replaced by the ρ mesons. The evolution factor is

$$E_e(t) = \alpha_s(t) a_1(t) \exp[-S_B(t) - S_\rho(t)], \quad (64)$$

with the Sudakov factor from the k_T resummation,

$$\exp[-S_\rho(\mu)] = \exp \left[-s(k_2^+, b_2) - s(P_2^+ - k_2^+, b_2) - 2 \int_{1/b_2}^\mu \frac{d\bar{\mu}}{\bar{\mu}} \gamma(\alpha_s(\bar{\mu})) \right], \quad (65)$$

and the hard scales,

$$t_e^{(1)} = \max(\sqrt{x_2}m_B, 1/b_1, 1/b_2), \quad t_e^{(2)} = \max(\sqrt{x_1}m_B, 1/b_1, 1/b_2). \quad (66)$$

The hard function is given by

$$\begin{aligned} h_e(x_1, x_2, b_1, b_2) = & S_t(x_2) K_0(\sqrt{x_1 x_2} m_B b_1) [\theta(b_1 - b_2) K_0(\sqrt{x_2} m_B b_1) I_0(\sqrt{x_2} m_B b_2) \\ & + \theta(b_2 - b_1) K_0(\sqrt{x_2} m_B b_2) I_0(\sqrt{x_2} m_B b_1)] . \end{aligned} \quad (67)$$

The Sudakov factor $S_t(x)$ arises from the threshold resummation of the double logarithms $\alpha_s \ln^2 x$, which are produced by the radiative corrections to the hard kernels. Its expression [51],

$$S_t(x) = \frac{2^{1+2c} \Gamma(3/2 + c)}{\sqrt{\pi} \Gamma(1 + c)} [x(1-x)]^c, \quad (68)$$

with the constant $c \sim 0.3$, provides further suppression in the end-point region of $x \rightarrow 0$, and improves the perturbative calculation. Since we have performed the leading-logarithm resummation so far, only the behavior of $S_t(x)$ at small x is reliable. The parametrization in the large x region, also vanishing, was proposed for convenience [51].

The numerical results are listed in Table 3, where diagram (a) [diagram (b)] refers to the lowest-order diagram with the hard gluon being on the B (ρ) meson side. It indicates that the next-to-leading-power corrections decrease (increase) the leading-power contribution from diagram (a) [diagram (b)] slightly. Considering the net effect, these corrections are indeed negligible.

	Diagram (a)	Diagram (b)	sum
Leading-power	0.330	0.088	0.418
Plus next-to-leading power	0.324	0.096	0.420

Table 3: Contributions to \mathcal{F}_L up to next-to-leading power.

4 COMMENTS ON PLAUSIBLE EXPLANATIONS

We now comment on the mechanism proposed in the literature to explain the abnormal polarization fractions of the $B \rightarrow \phi K^*$ decays. It will be argued that these proposals involve many free parameters, can not account for the polarizations of all $B \rightarrow VV$ modes simultaneously, or are too small to achieve the purpose. When discussing the annihilation effect on penguin-dominated decays, we found that the $B \rightarrow \rho K^*$ polarization data can be understood, which form the third category mentioned in the Introduction.

4.1 Annihilation Contribution

If the power-suppressed annihilation contribution from the $(S-P)(S+P)$ penguin operators is enhanced by some mechanism, one could have the different counting rules as shown in Eq. (2), and it might be possible to reach $R_L \sim 0.5$. This is the strategy adopted in [14], whose analysis was performed in the QCDF approach [15]. In QCDF an annihilation amplitude is not calculable due to the end-point singularity, and has to be formulated in terms of several free parameters, such as ρ_A . In the current case, different ρ_A have been introduced for the longitudinal and transverse polarization amplitudes in order to fit the data. These parameters greatly reduce the predictive power of QCDF. Because varying free parameters to explain the data can not be conclusive, we shall estimate the annihilation contribution in the PQCD approach, viewing that the PQCD predictions for the penguin annihilation are consistent with the measured direct CP asymmetries in $B^0 \rightarrow K^+\pi^-$, $\pi^+\pi^-$ [11, 12]. Such a calculation for a pure-penguin VV mode has been performed in [3]. As shown in Table 4, both the penguin annihilation and nonfactorizable contributions help reduce R_L . However, the combined effect is still not sufficient to lower the fractions R_L of the $B \rightarrow \phi K^*$ decays down to around 0.5.

Note that our predicted relative strong phases among A_L , A_{\parallel} , and A_{\perp} are consistent with the $B \rightarrow \phi K^{*0}$ data:

$$\begin{aligned} \phi_{\parallel} &= 2.21 \pm 0.22 \pm 0.05 \text{ (rad.)} , & \phi_{\perp} &= 2.42 \pm 0.21 \pm 0.06 \text{ (rad.)} [5] , \\ \phi_{\parallel} &= 2.34_{-0.20}^{+0.23} \pm 0.05 \text{ (rad.)} , & \phi_{\perp} &= 2.47 \pm 0.25 \pm 0.05 \text{ (rad.)} [6] . \end{aligned} \quad (69)$$

Table 4 also implies that R_L can decrease down to 0.75 for a pure-penguin VV mode, after taking into account the penguin annihilation and nonfactorizable contributions. Since the $B^+ \rightarrow \rho^+ K^{*0}$ decay is a pure-penguin process, and the ρ meson mass is not very different from the ϕ meson mass, the above PQCD analysis applies. Hence, we expect the longitudinal fraction $R_L \sim 0.75$ for the $B^+ \rightarrow \rho^+ K^{*0}$ decay, which is consistent with the Babar measurement, but a

bit larger than the Belle measurement. Due to the large uncertainty of the Belle data, there is in fact no discrepancy.

Mode	$ A_L ^2$	$ A_{\parallel} ^2$	$ A_{\perp} ^2$	$\phi_{\parallel}(rad.)$	$\phi_{\perp}(rad.)$
ϕK^{*0} (I)	0.923	0.040	0.035	π	π
(II)	0.860	0.072	0.063	3.30	3.33
(III)	0.833	0.089	0.078	2.37	2.34
(IV)	0.750	0.135	0.115	2.55	2.54
ϕK^{*+} (I)	0.923	0.040	0.035	π	π
(II)	0.860	0.072	0.063	3.30	3.33
(III)	0.830	0.094	0.075	2.37	2.34
(IV)	0.748	0.133	0.111	2.55	2.54

Table 4: (I) Without nonfactorizable and annihilation contributions, (II) add only nonfactorizable contribution, (III) add only annihilation contribution, (IV) add both nonfactorizable and annihilation contributions.

We then come to another mode $B^+ \rightarrow \rho^0 K^{*+}$, to which the tree operators contribute. Adopt the Babar measurement $R_L \sim 0.8$ for the $B^+ \rightarrow \rho^+ K^{*0}$ decay, and assume that the tree contribution, which obeys the counting rules in Eq. (1), affects only the longitudinal fraction. Hence, we simply add the color-allowed and color-suppressed tree amplitudes $T+C \sim 0.6 \exp(-90^\circ i)P$, which was extracted from the $B \rightarrow K\pi$ data [52], to the $B^+ \rightarrow \rho^+ K^{*0}$ longitudinal polarization amplitude P . The phase -90° has included the weak phase $\phi_3 \sim 60^\circ$. Without an explicit computation, we derive the polarization fractions for the $B^+ \rightarrow \rho^0 K^{*+}$ decay,

$$R_L \sim 0.86, \quad R_{\parallel} \sim R_{\perp} \sim 0.07, \quad (70)$$

which are consistent with the data within 1σ . We emphasize that we did not attempt a rigorous calculation of the $B \rightarrow \rho K^*$ decays here, which deserves a separate paper. In the perturbation theories, such as PQCD and QCDF, the factorizable $B \rightarrow \pi K$ amplitudes and the factorizable $B \rightarrow \rho K^*$ amplitudes with longitudinal polarizations are very similar. Small differences arise only from the meson masses and the distribution amplitudes. Therefore, the estimation using the three amplitudes from the $B \rightarrow \pi K$ modes, which have been available in the literature, makes sense.

The analysis and the result of the modes $B \rightarrow \omega K^*$ should be similar to those of $B \rightarrow \rho^0 K^*$. The explicit PQCD analysis of the $B \rightarrow \rho(\omega) K^*$ polarizations will be performed elsewhere. In conclusion, it is not difficult to accommodate the polarization data of the third category, the $B \rightarrow \rho K^*$ decays, within the Standard Model by means of the penguin annihilation and nonfactorizable contributions. It is also interesting to propose that the measurement of the $B \rightarrow \omega K^*$ polarizations can test the PQCD approach.

4.2 Charming Penguin

A charming penguin arises from the nonperturbative dynamics involved in a charm quark loop [53]. It is not calculable, has to be parameterized as a free parameter, and could be as large as a leading contribution. Recently, it has been introduced into soft-collinear effective theory (SCET) in order to account for the large $B \rightarrow \pi^0 \pi^0$ branching ratio [16]. The inputs of the measured CP asymmetries $S_{\pi\pi}$ and $A_{\pi\pi}$ demand a complex charming penguin, leading to a large penguin-over-tree ratio $|P/T| \sim 0.7$ [16]. With this P/T from the data, a large branching ratio $B(B^0 \rightarrow \pi^0 \pi^0) \sim 1.9 \times 10^{-6}$ was obtained. SCET does not attempt to explain why $|P/T|$ is so large, even though the Standard Model calculations based on PQCD and QCDF give $|P/T| = 0.23-0.29$. Another concern is that the $B \rightarrow \pi$ form factor from the data fitting is as small as 0.17 in the presence of the large charming penguin, in conflict with the values 0.28 from lattice QCD [54] and from light-cone sum rules [55, 56].

It has been also proposed that the charming penguin may be large enough to modify the counting rules in Eq. (1), and to explain the abnormal $B \rightarrow \phi K^*$ polarization data [16]. However, one also requires different free parameters for the different helicity amplitudes in order to lower the longitudinal polarization fraction, and to enhance the transverse polarization fractions. In this sense, SCET is similar to QCDF [14], where different ρ_A were introduced for the different helicity amplitudes. One needs different parameters for different modes too, such as $B \rightarrow \rho K^*$ and $B \rightarrow \phi K^*$. Our comment on SCET is then the same as on QCDF: the explanation by introducing as many parameters as necessary is always plausible, but can not be conclusive. We point out that the current SCET formalism is only of leading power: the chirally enhanced terms, proportional to m_0/m_B , have been dropped, and the annihilation (or W -exchange) amplitudes have not yet been formulated. We speculate that if the annihilation amplitude is included into SCET, the charming penguin may not be so essential. On the other hand, the charm-loop correction is well-behaved in perturbation theory without any infrared singularity, which has been known as the Bander-Silverman-Soni mechanism [57], implying that its nonperturbative piece is unlikely to be large. Besides, the light-cone-sum-rule analysis has supported a small charming penguin [58].

We have taken this chance to investigate the charm-quark loop correction to the $B \rightarrow \phi K^*$ polarization fractions in the PQCD approach. The gluon invariant mass attaching the charm-quark loop can be defined unambiguously as

$$q^2 = (1 - x_2)x_3 m_B^2 - |\mathbf{k}_{2T} - \mathbf{k}_{3T}|^2, \quad (71)$$

with x_2 and k_{2T} (x_3 and k_{3T}) being the momentum fraction and the transverse momentum in the K^* (ϕ) meson, respectively. It turns out that this effect increases R_L by about 5%, and is negligible. It also decreases the relative strong phases ϕ_{\parallel} and ϕ_{\perp} a bit.

4.3 Rescattering Effect

It has been proposed to explain the $B \rightarrow \phi K^*$ polarization data through the rescattering effect [17, 18, 19],

$$B \rightarrow D_s^{(*)} D^{(*)} \rightarrow \phi K^*. \quad (72)$$

The motivation is that the longitudinal polarization fraction of the intermediate states $D_s^* D^*$, as low as 0.5, might propagate into the final state ϕK^* . First, the massive B meson can decay into ϕK^* through many intermediate states. The analysis in [17, 18, 19] was restricted to only a few channels, and likely to be model-dependent [22]. The truncation of the higher intermediate states in this kind of analyses has been criticized [21]. Second, if this mechanism works for the $B \rightarrow \phi K^*$ modes, it will also work for $B \rightarrow \rho K^*$, which involve the same intermediate states. As obtained in [19], R_L of both the $B^+ \rightarrow \rho^+ K^{*0}$ and $B^+ \rightarrow \rho^0 K^{*+}$ decays are as low as 0.6. This observation is expected, since the additional tree amplitudes in the latter can not change R_L very much. However, the data in Table 1 indicate $R_L \sim 0.96$ for the $B^+ \rightarrow \rho^0 K^{*+}$ decay. In other words, the $B^+ \rightarrow \rho^0 K^{*+}$ polarization data, obeying the naive counting rules, have strongly constrained the rescattering effect. Third, the $D_s^* D$ and $D_s D^*$ intermediate states, contributing to the P -wave component, could affect the perpendicular polarization of the $B \rightarrow \phi K^*$ decays. Unfortunately, there exists a strong cancellation among these two channels due to the CP and SU(3) (CPS) symmetries [19]. The $D_s^* D^*$ intermediate state survives the CPS symmetry, which, however, exhibits a vanishing R_\perp as in Eq. (17). Therefore, the rescattering effect leads to the pattern,

$$R_L \sim R_\parallel \gg R_\perp, \quad (73)$$

contrary to the observed approximate equality $R_\parallel \approx R_\perp$.

Furthermore, it has been known that the $B \rightarrow KK$ decays are sensitive to rescattering effects. The $B \rightarrow KK$ branching ratios measured recently well agree with the PQCD predictions [59] as shown in Table 5, leaving very limited room for the rescattering effect. Note that no theoretical errors were presented in [59], since the detailed investigation of uncertainties in the PQCD approach was available only after Ref. [45]. Roughly speaking, the theoretical errors on PQCD predictions for branching ratios of two-body charmless B meson decays are about 30%. Viewing the contradiction of Eq. (73) to the $B \rightarrow \phi K^*$ polarization data, and the constraints from the measured $B^+ \rightarrow \rho^0 K^{*+}$ polarizations and from the measured $B \rightarrow KK$ branching ratios, we intend to conclude that the rescattering effect is not a satisfactory resolution to the polarization puzzle.

Branching Ratio	PQCD	Babar [60]
$B(B^+ \rightarrow K^+ K^0)$	1.65×10^{-6}	$(1.45_{-0.46}^{+0.53} \pm 0.11) \times 10^{-6}$
$B(B^0 \rightarrow K^0 \bar{K}^0)$	1.75×10^{-6}	$(1.19_{-0.35}^{+0.40} \pm 0.13) \times 10^{-6}$

Table 5: PQCD predictions for the CP-averaged $B \rightarrow KK$ branching ratios and the data.

4.4 Magnetic Penguin

If the $B \rightarrow \rho K^*$ data can be understood in the Standard Model by means of the penguin annihilation and nonfactorizable contributions, and only the $B \rightarrow \phi K^*$ decays exhibit an anomaly, it is natural to look for a unique mechanism for the latter. Such a mechanism, the

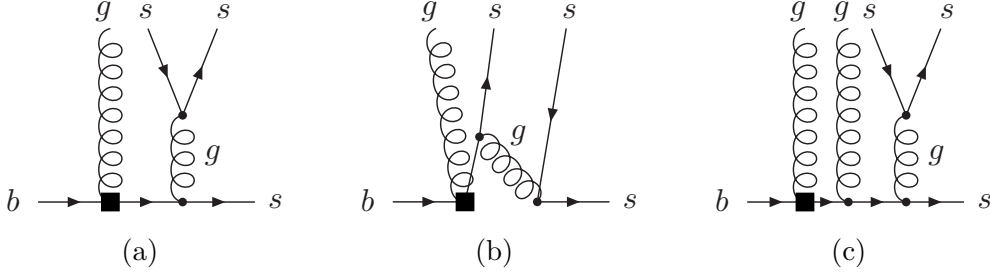


Figure 4: Some diagrams from the magnetic penguin which contribute to the transverse polarization fraction of the $B \rightarrow \phi K^*$ decays.

$b \rightarrow sg$ transition, has been proposed in [20]. The novel idea is that the transversely polarized gluon from the transition propagates into the ϕ meson, enhancing the transverse polarization amplitudes. The relevant matrix element was then parameterized in terms of a dimensionless free parameter κ . Assuming this parameter to be $\kappa \sim -0.25$, the authors of [20] claimed that the $B \rightarrow \phi K^*$ polarization data could be accommodated within the Standard Model. Similarly, varying a free parameter to fit the data can not be conclusive, and a reliable estimate of the κ value is necessary. As pointed out in [20], the same mechanism also contributes to the $B \rightarrow \omega K^*$ decays, and small $R_L \sim 0.5$ have been predicted. Therefore, the measurement of the $B \rightarrow \omega K^*$ polarizations will impose a stringent test on this proposal in the future. Note that PQCD postulates, contrary to [20], that R_L of the $B \rightarrow \omega K^*$ decays are as large as those of $B \rightarrow \rho^0 K^*$.

Besides the above experimental discrimination, we shall estimate the order of magnitude of κ in the framework of FA, following the method in [61]. The weak effective Hamiltonian contains the $b \rightarrow sg$ transition,

$$-\frac{G_F}{\sqrt{2}} V_{ts}^* V_{tb} C_{8g} O_{8g}, \quad (74)$$

with the magnetic penguin operator,

$$O_{8g} = \frac{g}{8\pi^2} m_b \bar{s}_i \sigma_{\mu\nu} (1 + \gamma_5) T_{ij}^a G^{a\mu\nu} b_j, \quad (75)$$

i, j being the color indices. The picture described in [20] is displayed in Fig. 4: one or more collinear gluons, emitted from the $B \rightarrow K^*$ form factor, produce the s and \bar{s} quarks in the color-octet state. They, together with the transversely polarized gluon from the $b \rightarrow sg$ transition, fragment into the color-singlet transversely polarized ϕ meson. According to this picture, we introduce three-parton distribution amplitudes to absorb the nonperturbative dynamics associated with the ϕ meson. Another diagram, in which the transversely polarized gluon produces the s and \bar{s} quarks and the collinear gluon flows into the ϕ meson directly, does not contribute, since the transverse polarization of the ϕ meson is mainly carried by its gluonic parton.

We first argue that the leading picture in Fig. 4(a), where the collinear gluon attaches the s quark from the $b \rightarrow sg$ transition, diminishes due to the G -parity. The corresponding

three-parton distribution amplitudes are defined via the matrix elements [32],

$$\begin{aligned} & \langle \phi(P_3, \epsilon_3^*(T)) | \bar{s}(-z) g G_{\mu\nu}(vz) \gamma_\alpha s(z) | 0 \rangle \\ &= -i P_{3\alpha} \left[P_{3\mu} \epsilon_{3\nu}^*(T) - \epsilon_{3\mu}^*(T) P_{3\nu} \right] f_{3\phi}^V \tilde{V}(v, P_3 \cdot z) , \end{aligned} \quad (76)$$

$$\begin{aligned} & \langle \phi(P_3, \epsilon_3^*(T)) | \bar{s}(-z) g \tilde{G}_{\mu\nu}(vz) \gamma_\alpha \gamma_5 s(z) | 0 \rangle \\ &= P_{3\alpha} \left[P_{3\nu} \epsilon_{3\mu}^*(T) - P_{3\mu} \epsilon_{3\nu}^*(T) \right] f_{3\phi}^A \tilde{A}(v, P_3 \cdot z) , \end{aligned} \quad (77)$$

with the dual gluon field strength tensor $\tilde{G}_{\mu\nu} = \epsilon_{\mu\nu\rho\sigma} G^{\rho\sigma}/2$. Other three-parton distribution amplitudes, irrelevant to the discussion below, are not quoted here. The Fourier transformation of the distribution amplitude \tilde{V} gives

$$\tilde{V}(v, P_3 \cdot z) = \int [dx] \exp[i P_3 \cdot z (x_{\bar{s}} - x_s + v x_g)] V(x_s, x_{\bar{s}}, x_g) , \quad (78)$$

with x_s , $x_{\bar{s}}$, and x_g being the momentum fractions carried by the s quark, the \bar{s} quark, and the gluon, respectively, and the integration measure,

$$\int [dx] \equiv \int_0^1 dx_{\bar{s}} \int_0^1 dx_s \int_0^1 dx_g \delta \left(1 - \sum_i x_i \right) . \quad (79)$$

The Fourier transformation of \tilde{A} is defined in the same way. The three-parton twist-3 vector meson distribution amplitudes have been also studied in [62]. The asymptotic models of V and A have been parameterized as [32, 63, 64]

$$V(x_s, x_{\bar{s}}, x_g) = 5040 (x_s - x_{\bar{s}}) x_s x_{\bar{s}} x_g^2 , \quad (80)$$

$$A(x_s, x_{\bar{s}}, x_g) = 360 x_s x_{\bar{s}} x_g^2 \left[1 + \omega_{1,0}^A \frac{1}{2} (7x_g - 3) \right] , \quad (81)$$

with the shape parameter $\omega_{1,0}^A = -2.1$. The antisymmetry (symmetry) of V (A) between the exchange of x_s and $x_{\bar{s}}$ is a consequence of the G -parity transformation in the SU(3) limit [32]. The constant $f_{3\phi}^V$ is chosen such that V is normalized according to

$$\int [dx] (x_s - x_{\bar{s}}) V(x_s, x_{\bar{s}}, x_g) = 1 . \quad (82)$$

We factorize the matrix element in Eq. (76) and the $B \rightarrow K^*$ transition form factor out of Fig. 4(a). The remaining part is the hard kernel, which must be symmetric under the exchange of x_s and $x_{\bar{s}}$. Therefore, Fig. 4(a), written as the convolution of the symmetric hard kernel with the antisymmetric three-parton distribution amplitude V , vanishes. The diagram with the collinear gluon attaching the b quark does not contribute, because its hard kernel is also symmetric. No matter how many infrared gluons are involved in the s - \bar{s} quark pair production, there is no contribution for the same reason. If factorizing the matrix element in Eq. (77) out of Fig. 4(a), it is easy to find that the corresponding hard kernel vanishes, because the s - \bar{s} quark pair does not form an axial-vector current. Therefore, we conclude that the leading diagram does not contribute to the transverse polarization amplitudes of the $B \rightarrow \phi K^*$ decays.

To survive the above suppressions, one has to consider subleading diagrams such as Fig. 4(b), in which both the s quark and the gluon from $b \rightarrow sg$ flow into the ϕ meson, or such as Fig. 4(c), in which one more infrared gluon fragments into the ϕ meson. For Fig. 4(b), an extra hard gluon is necessary for producing the $s\bar{s}$ quark pair, such that the price to pay is the α_s suppression. For Fig. 4(c), four-parton distribution amplitudes are involved, whose contribution is power-suppressed. We shall show that the order of magnitude of κ from Fig. 4(b) is, unfortunately, as small as 0.01, far away from $\kappa \sim -0.25$ required by the data. For simplicity, we analyze the contribution from the three-parton distribution amplitude V , and our conclusion applies to that from A . Due to the lack of the information of the four-parton twist-4 distribution amplitudes, we can not estimate the contribution from Fig. 4(c) in a reliable way. However, it is of higher power in m_ϕ/m_B , and unlikely to be huge.

Insert the Fierz identity,

$$I_{ij}I_{lk} = \frac{1}{4}(\gamma_\alpha)_{ik}(\gamma^\alpha)_{lj} + \cdots, \quad (83)$$

where the irrelevant terms have been suppressed, and the identity for color matrices,

$$I_{ij}I_{lk} = 2(T^b)_{ik}(T^b)_{lj} + \frac{1}{N_c}I_{ik}I_{lj}, \quad (84)$$

to change the fermion and color flows of the outgoing s and \bar{s} quarks, respectively. Figure 4(b), where the additional hard gluon attaches the s quark going into the K^* meson, is then factorized into

$$\begin{aligned} \mathcal{M} = & -\frac{G_F}{\sqrt{2}}V_{ts}^*V_{tb}\frac{g^2}{8\pi^2}m_bC_{8g}\int[dx]\text{IFT}\langle\phi(P_3,\epsilon_3^*(T))|\bar{s}(-z)gG^{a\mu\nu}(vz)T^b\gamma_\alpha s(z)|0\rangle \\ & \times \frac{1}{4}\text{tr}\left[\cdots\gamma^\lambda\gamma^\alpha\gamma_\lambda\frac{P_1-x_g}{(P_1-x_gP_3)^2}\not{P}_3\sigma_{\mu\nu}(1+\gamma_5)\cdots\right]\frac{2\text{tr}(T^cT^bT^cT^a)}{(P_2+x_{\bar{s}}P_3)^2}, \end{aligned} \quad (85)$$

where IFT means the inverse Fourier transformation. The indices λ denote the hard gluon vertices, and the dots in the trace represent the Feynman rules associated with the $B \rightarrow K^*$ form factor. Employing $2\text{tr}(T^cT^bT^cT^a) = -\delta^{ab}/(2N_c)$, Eq. (76) and Eq. (78), the above expression becomes

$$\begin{aligned} \mathcal{M} = & -\frac{G_F}{\sqrt{2}}V_{ts}^*V_{tb}\frac{g^2}{8\pi^2N_c}m_bC_{8g}f_{3\phi}^V\int[dx]V(x_s,x_{\bar{s}},x_g) \\ & \times \frac{1}{4}\text{tr}\left[\cdots\gamma^\lambda\not{P}_3\gamma_\lambda\frac{P_1-x_g}{(P_1-x_gP_3)^2}i\sigma_{\mu\nu}(1+\gamma_5)\cdots\right]\frac{P_3^\mu\epsilon_3^{*\nu}(T)}{(P_2+x_{\bar{s}}P_3)^2}. \end{aligned} \quad (86)$$

Neglecting the light meson masses, assuming $m_b \approx m_B$, and working out the product of the Dirac matrices in the trace, we derive

$$\begin{aligned} \mathcal{M} = & -\frac{G_F}{\sqrt{2}}V_{ts}^*V_{tb}\frac{\alpha_s}{4\pi N_c}C_{8g}\frac{f_{3\phi}^V}{m_B}\int[dx]\frac{V(x_s,x_{\bar{s}},x_g)}{x_{\bar{s}}(x_s+x_{\bar{s}})} \\ & \times \langle K^{*-}(P_2,\epsilon_2^*(T))|\bar{s}i\sigma_{\mu\nu}(1+\gamma_5)b|B^-(P_1)\rangle P_3^\nu\epsilon_3^{*\mu}(T). \end{aligned} \quad (87)$$

Comparing the above expression with Eq. (4) in [20], the parameter κ is given by

$$\kappa = \frac{\alpha_s}{4\pi N_c} \zeta_{3\phi}^V \int [dx] \frac{V(x_s, x_{\bar{s}}, x_g)}{x_{\bar{s}}(x_s + x_{\bar{s}})}, \quad (88)$$

with $\zeta_{3\phi}^V \equiv f_{3\phi}^V/(f_\phi m_\phi)$. For the values $\alpha_s = 0.4$ and $\zeta_{3\phi}^V = 0.013$ [32], and the model distribution amplitude in Eq. (80), we obtain $\kappa \approx 0.004$. Other diagrams with the hard gluon attaching the b quark and the transversely polarized gluon can be analyzed in a similar way, and the results are of the same order of magnitude. Adding these contributions leads to

$$\kappa \approx 0.01. \quad (89)$$

Hence, we intend to conclude that the magnetic penguin is not sufficient to resolve the $B \rightarrow \phi K^*$ puzzle.

5 CONCLUSION

In this paper we have investigated most of the $B \rightarrow VV$ modes carefully. Our observation is that the $B \rightarrow VV$ modes can be classified into four categories. For the tree-dominated decays, the polarization fractions are basically determined by kinematics. The upper part of Table 2 can be understood by kinematics in the heavy-quark limit. The longitudinal polarization fractions follow the mass hierarchy among the D_s^* , D^* and ρ (K^*) mesons. The lower part of Table 2 can be understood by kinematics in the large-energy limit. We always have $R_L \sim 1$ for the decays into two light vector mesons. It has been found that the above simple kinematic estimates in the heavy-quark and large-energy limits are robust under subleading corrections. For this part, we have analyzed the next-to-leading-power corrections to the universal IW function, the nonfactorizable contributions, the two-parton twist-4 contributions, and part of next-to-leading-order contributions from the charm-quark loop, all of which are negligible. That is, QCD dynamics plays only a minor role for the polarizations of the tree-dominated decays.

As a byproduct, we have predicted the longitudinal polarization fractions of the $B^+ \rightarrow (D_s^{*+}, D^{*+})\rho^0$ modes in the large-energy limit using FA, and found $R_L \sim 0.7$. We have also calculated the polarization fractions of the $B^0 \rightarrow \bar{D}^{*0}D^{*0}$ decay explicitly in the PQCD approach based on k_T factorization theorem. The result $R_L \sim 1$ is quite different from R_L of other $B \rightarrow D^*D^*$ modes, since it is dominated by the nonfactorizable W -exchange topology. The above predictions can be confronted with the future data.

For the penguin-dominated modes, the polarization fractions can deviate from the naive counting rules based on kinematics, because of the important annihilation contribution from the $(S - P)(S + P)$ operators. This mechanism explains the third category listed in the lower part of Table 1: R_L can decrease to 0.75 for the $B^+ \rightarrow \rho^+ K^{*0}$ mode. Adding the tree contribution, R_L of the $B^+ \rightarrow \rho^0 K^{*+}$ decay can go up to about 0.9. We have postulated from the viewpoint of PQCD that the $B \rightarrow \omega K^*$ decays also belong to the third category, and should show R_L similar to those of $B \rightarrow \rho^0 K^*$. All the above three categories can be accommodated within the Standard Model. Only the fourth category, the $B \rightarrow \phi K^*$ decays, can not. They are dominated by the penguin contribution, but their $R_L \sim 0.5$ are much lower than 0.75. We have carefully analyzed the various mechanism proposed in the literature to resolve this anomaly,

and concluded that none of them is satisfactory. Therefore, the $B \rightarrow \phi K^*$ polarization data remain as a puzzle. However, we emphasize that we are not claiming a signal of new physics, since the complicated QCD dynamics in the $B \rightarrow VV$ decays has not yet been fully explored. For example, a smaller $B \rightarrow K^*$ form factor A_0 could decrease R_L significantly [65].

We thank C. Bauer, I.I. Bigi, P. Chang, C.H. Chen, K.F. Chen, H.Y. Cheng, C.K. Chua, W.S. Hou, Y.Y. Keum, Z. Ligeti, M. Nagashima, D. Pirjol, A.I. Sanda, and I. Stewart for useful discussions. This work was supported by the National Science Council of R.O.C. under Grant No. NSC-93-2112-M-001-014, by the Taipei Branch of the National Center for Theoretical Sciences of R.O.C., and by the Grants-in-aid from the Ministry of Education, Culture, Sports, Science and Technology, Japan under Grant No. 14046201. HNL acknowledges the hospitality of Department of Physics, Tohoku University, where this work was initiated.

References

- [1] J. Zhang *et al.* [BELLE Collaboration], Phys. Rev. Lett. **91**, 221801 (2003).
- [2] B. Aubert *et al.* [BABAR Collaboration], Phys. Rev. Lett. **91**, 171802 (2003).
- [3] C.H. Chen, Y.Y. Keum, and H-n. Li, Phys. Rev. D **66**, 054013 (2002).
- [4] H-n. Li, hep-ph/0408232.
- [5] K. Abe, *et al.* [BELLE Collaboration], hep-ex/0408141.
- [6] B. Aubert *et al.* [BABAR Collaboration], Phys. Rev. Lett. **93**, 231804 (2004).
- [7] K. Abe *et al.* [Belle Collaboration], hep-ex/0408102.
- [8] B. Aubert *et al.* [BABAR Collaboration], hep-ex/0408093.
- [9] M. Bauer, B. Stech, M. Wirbel, Z. Phys. C **29**, 637 (1985); *ibid.* **34**, 103 (1987).
- [10] N. Isgur and M.B. Wise, Phys. Lett. B **232**, 113 (1989); **237**, 527 (1990).
- [11] Y.Y. Keum, H-n. Li, and A.I. Sanda, Phys. Lett. B **504**, 6 (2001); Phys. Rev. D **63**, 054008 (2001); Y.Y. Keum and H-n. Li, Phys. Rev. **D63**, 074006 (2001).
- [12] C. D. Lü, K. Ukai, and M. Z. Yang, Phys. Rev. D **63**, 074009 (2001); C.D. Lü and M.Z. Yang, Eur. Phys. J. C **23**, 275 (2002).
- [13] Y. Grossman, Int. J. Mod. Phys. A **19**, 907 (2004).
- [14] A. Kagan, Phys. Lett. B **601**, 151 (2004); hep-ph/0407076.
- [15] M. Beneke, G. Buchalla, M. Neubert, and C.T. Sachrajda, Phys. Rev. Lett. **83**, 1914 (1999); Nucl. Phys. **B591**, 313 (2000); Nucl. Phys. **B606**, 245 (2001).

- [16] C.W. Bauer, D. Pirjol, I.Z. Rothstein, and I.W. Stewart, Phys. Rev. D **70**, 054015 (2004).
- [17] P. Colangelo, F. De Fazio, and T.N. Pham, Phys. Lett. B **597**, 291 (2004).
- [18] M. Ladisa, V. Laporta, G. Nardulli, and P. Santorelli, Phys. Rev. D **70**, 114025 (2004).
- [19] H.Y. Cheng, C.K. Chua, and A. Soni, Phys. Rev. D **71**, 014030 (2005); H.Y. Cheng, hep-ph/0410314.
- [20] W.S. Hou and M. Nagashima, hep-ph/0408007.
- [21] L. Wolfenstein, hep-ph/0407344.
- [22] Z. Ligeti, hep-ph/0408267.
- [23] S. Eidelman *et al.* [Particle Data Group Collaboration], Phys. Lett. B **592**, 1 (2004).
- [24] T. Aushev, Belle-conf-0453, talk presented at the 32nd International Conference on High Energy Physics, Aug. 16-22, 2004, Beijing, China.
- [25] B. Aubert *et al.* [BABAR Collaboration], Phys. Rev. Lett. **91**, 131801 (2003).
- [26] B. Aubert *et al.* [BABAR Collaboration], Phys. Rev. Lett. **92**, 141801 (2004).
- [27] B. Aubert *et al.* [BABAR Collaboration], Phys. Rev. Lett. **93**, 231801 (2004); Phys. Rev. D **69**, 031102 (2004).
- [28] B. Aubert *et al.* [BABAR Collaboration], hep-ex/0409059.
- [29] J.L. Rosner, Phys. Rev. D **42**, 3732 (1990).
- [30] M. Beneke and T. Feldmann, Nucl. Phys. **B592**, 3 (2000).
- [31] J. Charles *et al.*, Phys. Rev. D **60**, 014001 (1999).
- [32] P. Ball, V.M. Braun, Y. Koike, and K. Tanaka, Nucl. Phys. **B529**, 323 (1998).
- [33] T. Kurimoto, H.-n. Li, and A.I. Sanda, Phys. Rev. D **67**, 054028 (2003).
- [34] Y.Y. Keum, T. Kurimoto, H.-n. Li, C.D. Lu, and A.I. Sanda, Phys. Rev. D **69**, 094018 (2004).
- [35] J. Botts and G. Sterman, Nucl. Phys. **B325**, 62 (1989).
- [36] H.-n. Li and G. Sterman, Nucl. Phys. **B381**, 129 (1992).
- [37] C.H. Chen, Y.Y. Keum, and H.-n. Li, Phys. Rev. D **64**, 112002 (2001).
- [38] H.-n. Li, Phys. Rev. D **64**, 014019 (2001); M. Nagashima and H.-n. Li, hep-ph/0202127; Phys. Rev. D **67**, 034001 (2003).

- [39] C.Y. Wu, T.W. Yeh, and H-n. Li, Phys. Rev. D **53**, 4982 (1996); T.W. Yeh and H-n. Li, Phys. Rev. D **56**, 1615 (1997).
- [40] Y. Li, C.D. Lu, and Z.J. Xiao, J. Phys. G **31**, 273 (2005).
- [41] M. Neubert, Phys. Lett. B **306**, 357 (1993); Nucl. Phys. **B416**, 786 (1994); M. Luke, Phys. Lett. B **252**, 447 (1990); C.G. Boyd and B. Grinstein, Nucl. Phys. **B451**, 177 (1995).
- [42] H-n. Li and H.L. Yu, Phys. Rev. Lett. **74**, 4388 (1995); Phys. Lett. B **353**, 301 (1995); Phys. Rev. D **53**, 2480 (1996).
- [43] H-n. Li and H.S. Liao, Phys. Rev. D **70**, 074030 (2004).
- [44] M. Bauer and M. Wirbel, Z. Phys. **C42**, 671 (1989).
- [45] T. Kurimoto, H-n. Li, and A.I. Sanda, Phys. Rev. D **65**, 014007 (2002).
- [46] H. Kawamura, J. Kodaira, C.F. Qiao, and K. Tanaka, Phys. Lett. B **523**, 111 (2001); Mod. Phys. Lett. A **18**, 799 (2003).
- [47] Z.T. Wei and M.Z. Yang, Nucl. Phys. **B642**, 263 (2002); C.D. Lu and M.Z. Yang, Eur. Phys. J. C **28**, 515 (2003).
- [48] B. Aubert *et al.* [BABAR Collaboration], hep-ex/0408040.
- [49] A. Datta and D. London, Phys. Lett. B. **584**, 81 (2004); J. Albert, A. Datta, and D. London, Phys. Lett. B **605**, 335 (2005).
- [50] P. Ball and V.M. Braun, Nucl. Phys. **B543**, 201 (1999).
- [51] H-n. Li, Phys. Rev. D **66**, 094010 (2002); K. Ukai and H-n. Li, Phys. Lett. B **555**, 197 (2003).
- [52] Y.Y. Charng and H-n. Li, Phys. Lett. B. **594**, 185 (2004); Phys. Rev. D **71**, 014036, (2005).
- [53] M. Ciuchini, E. Franco, G. Martinelli, and L. Silvestrini, Nucl. Phys. **B501**, 271 (1997); M. Ciuchini, R. Contino, E. Franco, G. Martinelli, and L. Silvestrini, Nucl. Phys. **B512**, 3 (1998); Erratum-ibid. **531**, 656 (1998).
- [54] D. Becirevic, hep-ph/0211340.
- [55] A. Khodjamirian *et al.*, Phys. Lett. B **410**, 275 (1997); A. Khodjamirian and R. Ruckl, Phys. Rev. D **58**, 054013 (1998).
- [56] P. Ball J. High Energy Phys. **09**, 005 (1998).
- [57] M Bander, D. Silverman, and A. Soni, Phys. Rev. Lett. **43**, 242 (1979).
- [58] A. Khodjamirian, Th. Mannel, and B. Melic, Phys. Lett. B **571**, 75 (2003); Phys. Lett. B **572**, 171 (2003).

- [59] C.H. Chen and H-n. Li, Phys. Rev. D **63**, 014003 (2001).
- [60] B. Aubert *et al.* [BABAR Collaboration], hep-ex/0408080.
- [61] C.H. Chen and H-n. Li, Phys. Rev. D **69**, 054002 (2004).
- [62] I. Halperin, Phys. Rev. D **57**, 1680 (1998).
- [63] V.L. Chernyak and A.R. Zhitnitsky, Phys. Rep. **112**, 173 (1984)
- [64] M.A. Shifman, A.I. Vainshtein, and V.I. Zakharov, Nucl. Phys. **B147**, 385; 448; 519, (1979).
- [65] H-n. Li, hep-ph/0411305.